THE ASTROPHYSICAL JOURNAL, 463:681–693, 1996 June 1

MULTIPLE SCATTERING IN CLUMPY MEDIA. I. ESCAPE OF STELLAR RADIATION FROM A CLUMPY SCATTERING ENVIRONMENT

ADOLF N. WITT AND KARL D. GORDON
Ritter Astrophysical Research Center, The University of Toledo, Toledo, OH 43606
Received 1995 July 24; accepted 1995 December 28

ABSTRACT

We studied the radiative transfer in a spherical, two-phase clumpy medium, in which coherent, nonconservative scattering is the dominant opacity source and where the source of photons is situated at the center. The structure of the medium is random but statistically homogeneous and is characterized by the density ratio between the low- and high-density phases, the optical depth radius of the equivalent homogeneous dust distribution, the filling factor of high-density clumps, and the length scale of individual clumps. We examined in detail the cloud mass spectrum, the distribution of optical depths, and the apparent fractal nature of the projected cloud structures. The photometric characteristics of the clumpy scattering system are studied as a function of density contrast between the two phases, of the filling factor, and of the length scale of high-density clumps, and they are compared with those of homogeneous, constant-density distributions of equal effective optical depth. Direction-averaged surface brightness distributions of the scattered light are studied for both optically thick and optically thin cases, which reveal the important role of scattering by the optically thin interclump medium. The conversion of UV/optical/near-IR radiation into thermal far-IR dust radiation in a dusty system is profoundly affected by the structure of the medium; the homogeneous, constant-density distribution always provides the highest conversion efficiency for any given geometry and dust mass. The effective optical depth of a clumpy distribution is known not to scale linearly with the equivalent optical depth of a homogeneous distribution of equal dust mass; this leads to effective attenuation laws that differ from the original opacity law assumed for the dust in the system. The expected reddening is substantially reduced for clumpy media. Finally, since the scattering response of a clumpy system is consistently that of an equivalent system of lower effective optical depth and lower effective albedo, efforts to determine the dust albedo of real systems with clumpy dust distributions by employing models, which are homogeneous, can lead to a bias toward albedo values that are too low.

Subject headings: dust, extinction — radiative transfer

1. INTRODUCTION

One of the most profound characteristics of diffuse media in the universe is their structure. In particular, the interstellar medium in spiral and irregular galaxies reveals itself to a wide assortment of observational techniques as a highly structured environment on a large range of scales, with density contrasts ranging over many orders of magnitude (see, e.g., Colomb, Pöppel, & Heiles 1980; Scalo 1990; Rosen & Bregman 1995).

Dust in the interstellar medium provides the dominant source of opacity to stellar photons with energies $E < 13.6$ eV, while atomic hydrogen in interstellar space controls the radiative transfer of stellar photons with $E \geq 13.6$ eV. In molecular clouds, absorption by molecular hydrogen in the range $11.2 \text{ eV} \leq E \leq 13.6$ eV is a significant competitor to dust as an opacity source. It is important, therefore, to ask how the structure of the medium affects the escape of stellar radiation from systems that consist of stellar sources and a structured, diffuse medium. In this paper, we will consider photons with $E < 11.2$ eV only, so that scattering and absorption by dust are the principal opacity sources.

Past treatments of this problem have been concerned with the subject of reddening of light from extended sources, e.g., H II regions, by a thick, inhomogeneous dust layer (Natta & Panagia 1984) and the transfer of an external radiation field through a plane-parallel clumpy dust layer (Boissé 1990, 1991; Hobson & Scheuer 1993; Hobson & Padman 1993; Spaans 1994), representing a photodissociation front. While Natta & Panagia (1993) treated the extinction by a clumpy screen with a zero-density interclump medium, excluding scattering, Boissé (1990) and Hobson & Scheuer (1993) provided the full radiative transfer solutions for a two-phase and N-phase slab, respectively, although only with isotropic scattering. Boissé (1990) also gave an extensive introduction to related formal studies of radiative transfer through cloudy atmospheres or particle transfer through two-phase media occurring in inertial confinement fusion applications, and this will not be repeated here.

Past application in astrophysics of models involving radiative transfer in clumpy media have concerned mainly photodissociation regions (see, e.g., Meixner & Tielens 1993). Observations of submillimeter and far-infrared atomic fine-structure and molecular rotation lines in such regions suggest that interfaces between atomic and molecular gas phases are simultaneously composed of high-density gas and yet are relatively translucent to the exciting UV radiation. Only a clumpy medium can fulfill both conditions at the same time (Stutzki et al. 1991; Howe et al. 1991; Burton, Hollenbach, & Tielens 1990; Falgarone, Phillips, & Walker 1991; Stacey et al. 1993; Spaans 1994).

Our interest in this topic is guided mainly by applications in which the escape of stellar radiation from systems with clumpy scattering media is involved. Examples are reflection nebulae and galaxies rich in interstellar matter, primarily spirals and starburst systems. Observations of

reflection nebulae at near-infrared wavelengths (see, e.g., Sellgren, Werner, & Dinerstein 1992) show that models based on homogeneous dust distributions fail to explain simultaneously the surface brightness levels observed at optical/UV wavelengths and at near-IR wavelengths. Two-phase clumpy models, in which the low-density interclump medium primarily scatters the short-wavelength photons and the high-density clumps mainly scatter the near-infrared light, are a possible solution. Similarly, the problems of internal extinction in galaxies and the conversion of stellar radiation into far-infrared thermal emission from dust are of great current interest. While it is well known that the interstellar medium in galaxies is highly structured, the models designed to deal with problems of internal dust in galaxies so far have been based on homogeneous distributions (see, e.g., Bruzual, Magris, & Calvet 1988; Witt, Thronson, & Capuano 1992b; Byun, Freeman, & Kylafis 1994). Consequently, estimates of the typical opacity of spiral disk galaxies based on such homogeneous distribution models (see, e.g., Cunow 1992; Valentijn 1994; Byun 1993; Jansen et al. 1994; Huizinga & van Albada 1992; Bosma et al. 1992; Han 1992; Rowan-Robinson 1992) may lead to incorrect conclusions concerning the actual mass of dust present in these systems. Indeed, Block et al. (1994), in their effort to estimate dust masses in face-on spirals based on the interpretation of $V-K$ or $B-K$ color excesses, stress repeatedly that their results are lower limits to the true dust masses because the effective opacity of a clumpy dust distribution will be less than that of a homogeneous distribution of the same dust mass. We will emphasize the comparison of clumpy scattering systems with homogeneous ones possessing the same mass and homogeneous ones exhibiting the same effective optical depth in order to allow quantitative assessments of the effects of clumpiness.

The escape of radiation from dusty systems with embedded sources, such as reflection nebulae and dusty galaxies, is strongly affected by the form of the scattering phase function. Recent studies of the phase function asymmetry (Witt, Oliveri, & Schild 1990; Witt et al. 1992a, 1993; Calzetti et al. 1995) have shown that the deviation from isotropy of scattering is severe and increasing toward the far-ultraviolet. Values of the phase function asymmetry g range from $g \approx 0.6$ to $g \approx 0.8$, invalidating some of the conclusions of Witt (1988), which were based on earlier, more limited data. Analytical approaches to the radiative transfer problem in clumpy media (Boissé 1990; Hobson & Scheuer 1993) provide solutions for the isotropic case ($g = 0.0$) only. By contrast, the Monte Carlo method permits radiative transfer calculations for arbitrary values of g and arbitrarily complex geometries. Since our ultimate goal is the interpretation of multiwavelength observations of reflection nebulae and late-type galaxies, which includes the aim of determining dust scattering properties from the far-UV to the near-IR, we decided to employ the Monte Carlo method for the current study.

In this paper, we will examine the simplest type of system with embedded sources, that of a spherical cloud containing a two-phase medium with a single central source. In a subsequent contribution, systems with extended star distributions will be examined. We will describe the current model and characterize the statistical properties of the scattering clumpy medium in § 2. In § 3, we will present detailed model results, followed by a discussion in § 4, and a summary of results in § 5.

2. THE MODEL

2.1. *Model Geometry*

We constructed a statistically homogeneous clumpy environment by dividing a cubical volume into N^3 cubical bins, typically with $N = 10$–50. Each individual bin is assigned randomly to either a high-density state or a low-density state by a Monte Carlo process. The size of a bin relative to the size of the ensemble represents the smallest length scale of density inhomogeneity which is taken into account in this model. A filling factor, *ff*, for high-density bins determines the statistical frequency of the bins in the two states. We typically considered a range of filling factors from 0.01 to 0.40, which covers the extent of physical environments ranging from the case of having rare, single high-density clumps in an extended medium to the case in which the high-density medium forms an interconnected porous structure, with voids filled by a low-density medium. The probability of any of the N^3 bins being in a high-density state or a low-density state is independent of the state of adjacent bins and independent of location within the cubical volume in general. The medium can therefore be described as statistically homogeneous but clumpy. The random occurrence of high-density clumps in adjacent bins leads to a distribution of connected clumps with a well-determined size and mass spectrum. The formal theory that describes the statistical properties of systems like the one defined here is percolation theory (see, e.g., Stauffer 1985). We will discuss the properties of our system within the context of this theory in § 2.2.3 and subsequent sections.

Our most thoroughly studied case is that of "constant mass." Because of the randomness of the assignment of density phase to a bin, the constant mass assumption is not strict but, rather, is subject to small fluctuations. These fluctuations may become more significant, especially in cases of small filling factors and high density contrast. As the density ratio between the low-density and high-density phases (k_2/k_1) is varied, in our cases over a range $1.0 \geq k_2/k_1 \geq 0.001$, the amount of mass allocated to individual bins of either phase is then determined by the filling factor of high-density bins. Both phases of the medium are considered occupied by dust grains of constant albedo, which scatter according to the nonisotropic Henyey & Greenstein (1941) phase function. For this paper, we assumed that the albedo is the same in both density phases and has the value of $a = 0.6$. This value is fairly representative of empirically determined dust albedos over most of the ultraviolet to near-infrared spectral range (Gordon et al. 1994). For the phase function asymmetry, we assumed $g = 0.6$, typical of the strongly forward-directed scattering patterns expected for wavelength-sized grains in the interstellar medium (see, e.g., Calzetti et al. 1995). Valid arguments can be made for considering differences in grain properties in high-density clumps compared to the low-density interclump medium (Boissé 1991), and our model is capable of accommodating such situations. However, such variations would confuse the study of purely the effects of structure on the transfer of radiation and are therefore not considered here.

Photons are assumed to originate in a centrally located, isotropically radiating point source. The transfer of individual photons through the clumpy structure is followed using a Monte Carlo approach (Witt 1977a; Audic & Frisch 1993), and the classification of photons according to their status (n-times scattered or direct, direction, and weight) is

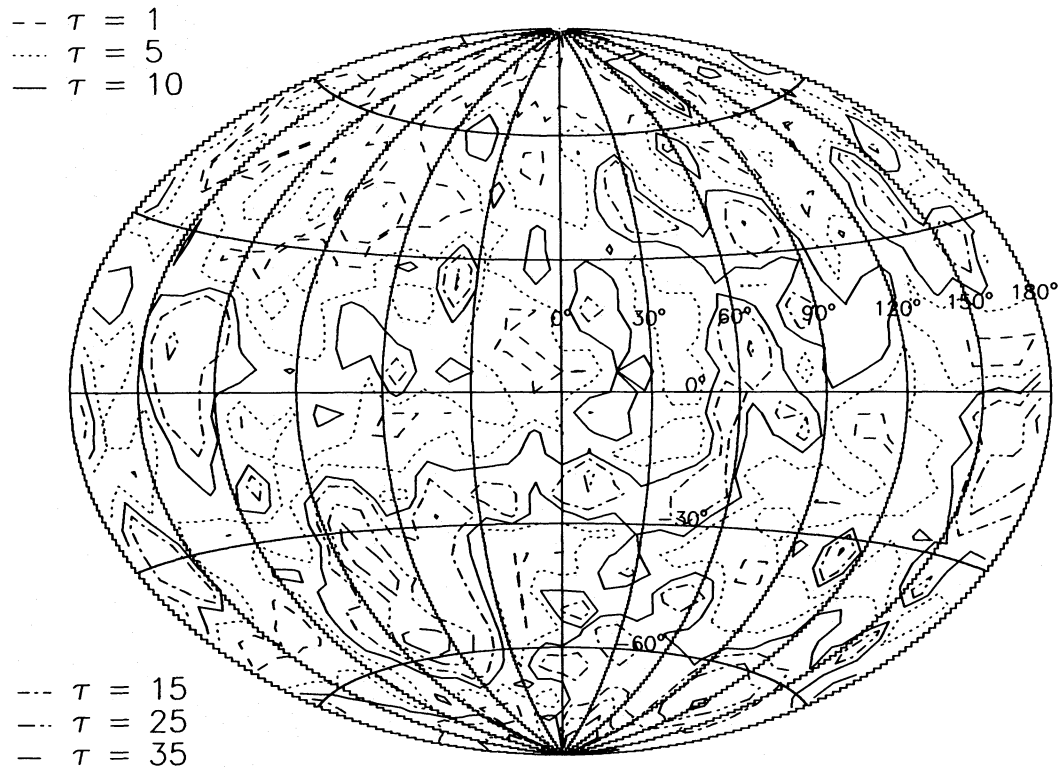

FIG. 1.—Aitoff equal-area projection of the distribution of the line-of-sight optical depths as a function of direction, as seen by the central source. The radial optical depth for the equivalent homogeneous constant density dust distribution is $\tau_H = 10$. The clumpy case illustrated here is for the case of $ff = 0.10$, $k_2/k_1 = 0.01$, and $N = 20$.

carried out at a spherical surface with a radius equal to $N/2$ bin lengths, i.e., a sphere inscribed within the boundaries of the original cubical volume. We obtain quantities such as the average flux of direct starlight seen by an outside observer, the integrated nebular flux, and the radial surface brightness distribution of scattered light by averaging over many lines of sight distributed randomly over all directions.

2.2. *Characterization of the Clumpy Medium*

2.2.1. *Optical Depth Distribution and the Effective Optical Depth*

As a consequence of the clumpy distribution, in general any two random lines of sight from the central source to the spherical surface may represent different optical thicknesses to escaping photons. In Figure 1, we present one example of the distribution of radial optical depths as seen by the central source, shown here in an Aitoff equal-area projection. This case represents an amount of dust with an equivalent radial optical depth $\tau_H = 10$ in a homogeneous constant density distribution. Here, however, we show the case of $ff = 0.10$, $k_2/k_1 = 0.01$, and $N = 20$. This implies that the optical thickness of each high-density bin is $\tau_1 \approx 10$; the optical thickness of each interclump medium bin is $\tau_2 \approx 0.1$. Consequently, the maximum optical depth along any line of sight cannot exceed $\tau \approx 100$ and cannot fall below $\tau = 1.00$. The actual distribution of optical depths along a large number of random radii is shown in Figure 2. Indeed, $\tau \approx 1.00$ corresponds to the numerous lines of sight that exclusively penetrate the interclump medium, while the actual maximum of $\tau \approx 40$ corresponds to the lines of sight penetrating four clumps. Lines of sight penetrating more than four dense clumps were not encountered in this case with $ff = 0.10$.

The effective optical depth $\tau_{\rm eff}$ of the clumpy dust distribution shown in Figure 1 can be obtained from $\tau_{\rm eff} = -\ln(L_{\rm AT}/L_*)$, where $L_{\rm AT}$ is the attenuated, nonscattered stellar flux integrated over the outer surface, and L_* is the original stellar luminosity. While $\tau_{\rm eff}$ is not measurable by a single observer at the wavelength for which it is defined, a measurement of the total infrared luminosity of the entire system can provide a basis for a good estimate of $\tau_{\rm eff}$. We show the effective optical depth $\tau_{\rm eff}$ as a function of k_2/k_1, for a range of filling factors in Figure 3, for the case in which the initial optical depth for the homogeneous case is $\tau_H = 10$ and in which the mass remains constant within the limits defined in § 2.1. The effective optical depth of the case illus-

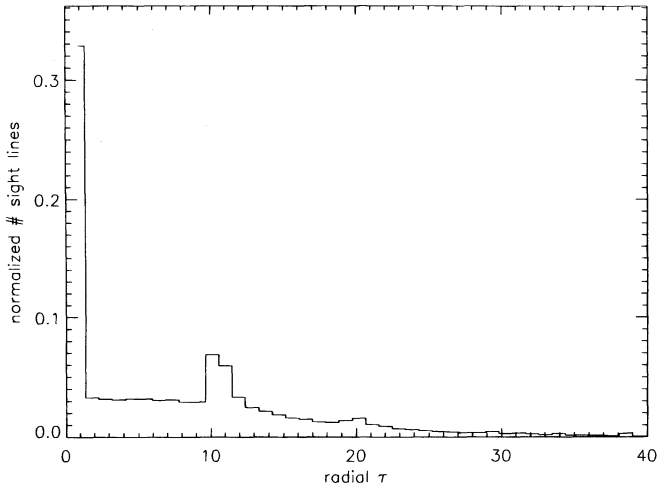

FIG. 2.—Frequency spectrum of optical depths, as encountered by random photons isotropically emitted by the central source in the clumpy distribution illustrated in Fig. 1.

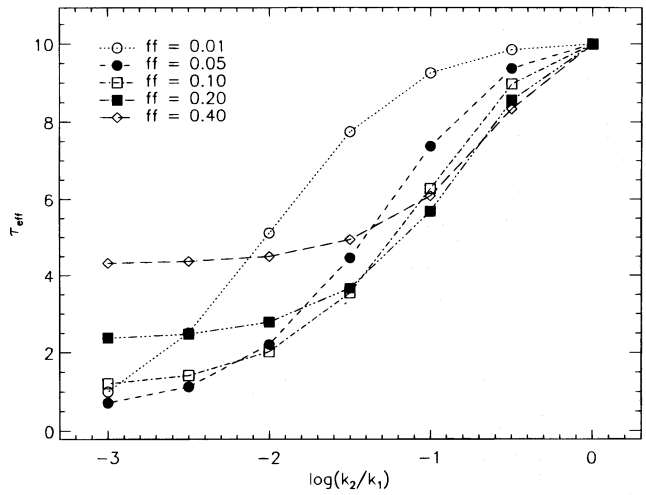

FIG. 3.—Effective optical depth of a clumpy distribution with $\tau_H = 10$ and $N = 20$ as a function of the density ratio of interclump-to-clump media, k_2/k_1. The range of filling factors ff is designed to illustrate the varying importance of the interclump medium in relation to the clumps. All models presented have equal masses of dust.

trated in Figure 1 ($ff = 0.1$, $k_2/k_1 = 0.01$) turns out to be $\tau_{eff} \approx 2$. When compared to the opacity of the homogeneous case of $\tau_H = 10$, this represents an increase in transparency by about a factor of 3×10^3 for the same dust mass. This result is consistent with numerical and analytical results presented by Boissé (1990, Fig. 3*a*) and Hobson & Scheuer (1993, Fig. 3), considering that slightly different values for the dust albedo were assumed in the three cases and that our result applies to $g = 0.6$, while the others were done for $g = 0.0$.

2.2.2. *Role of the Interclump Medium*

Figure 3 reveals the changing roles of clumps and the interclump medium in controlling the transfer of escaping stellar radiation. In the limit in which k_2/k_1 is near unity, the effective optical depth is determined by the extinction coefficient of the interclump medium. This is illustrated by Figure 4, which shows the optical thickness τ_2 per bin of interclump medium. The optical thickness τ_2 is largest for the smallest filling factor, at any k_2/k_1. Initially, the effective optical depth of the system (Fig. 3) follows the same trend for ratios k_2/k_1 near unity, e.g., $\log(k_2/k_1) > -0.5$. As the density ratio decreases, this trend is reversing, beginning with the highest filling factors. The opacity of the clumps, which increases with decreasing density ratio, begins to dominate the radiative transfer.

In the limit of large density contrasts between the clumps and the interclump medium, e.g., $\log(k_2/k_1) < -3.0$, the effective optical thickness of the system is essentially determined by the clump filling factor, as long as the optical depth per clump is substantial. In Figure 5 we show the computed optical thickness τ_1 of clumps as a function of k_2/k_1 for a range of filling factors $0.01 \leq ff \leq 0.4$ for the same constant mass case of $\tau_H = 10$. While the clump optical thicknesses τ_1 for $k_2/k_1 = 0.001$ for $ff = 0.4$, 0.2, and 0.1 vary in the ratio 1:2:4, the resulting effective optical depths τ_{eff} shown in Figure 3 vary more nearly in the ratio 4:2:1, i.e., in the ratio of the filling factors, demonstrating that simple blocking of radiation, which is proportional to the filling factor, is the principal source of opacity in this limit. This suggests that in a real astrophysical environment, both the filling factor of clumps and the density contrast between clumps and the interclump medium will be important parameters.

2.2.3. *Cloud Mass Spectrum*

Our clump production process is random with respect to the spatial coordinates of individual clumps. As the filling factor of clumps is allowed to increase, the likelihood that spatially adjoining bins are occupied by clumps increases as well, which leads to the appearance of complex cloud structures composed of one or more connected clumps. Two clumps are considered connected when they share one entire side. As the filling factor ff exceeds the percolation threshold for a simple cubic structure ($ff \approx 0.25$), clumps begin to be part of a single interconnected structure with low-density pores (Stauffer & Aharony 1992).

Recent attempts to determine the volume filling factor for interstellar clouds in the solar neighborhood of the Galaxy (van Buren 1989; Murthy, Walker, & Henry 1992; Gaustad & van Buren 1993) have resulted in mutually exclusive results. Gaustad & van Buren (1993) found $ff = 14.6\% \pm 2.4\%$, while Murthy et al. (1992) claimed

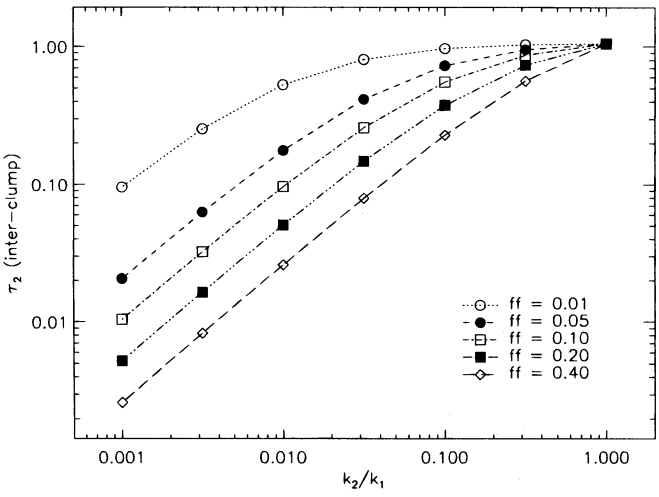

FIG. 4.—Optical depth τ_2 per bin of interclump medium for the cases illustrated in Fig. 3.

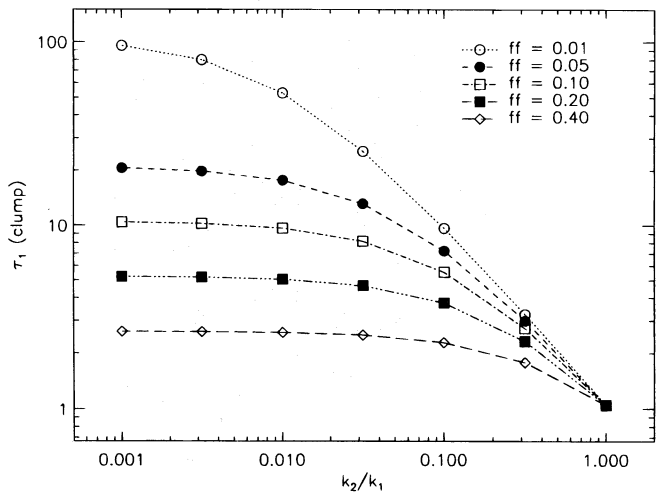

FIG. 5.—Optical depth τ_1 per bin of clump medium for the cases illustrated in Fig. 3.

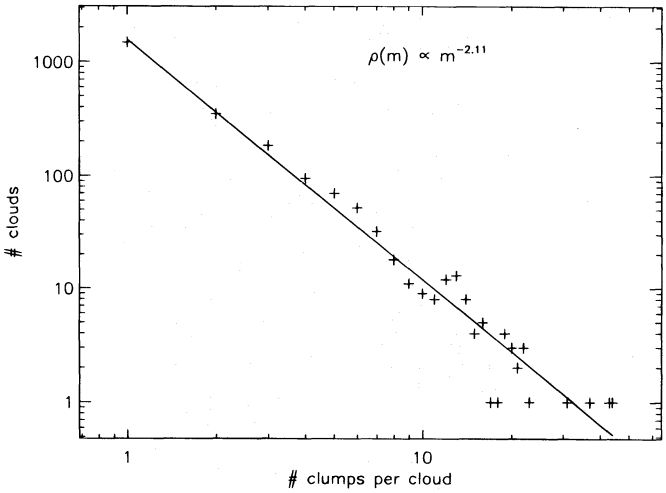

FIG. 6.—Clumps vary in size and mass through the sharing of one face between adjacent high-density bins. The distribution of clumps with varying number of high-density bins is shown here for the case of $N = 20$ and a filling factor $ff = 0.2$. This distribution is similar to the mass spectrum of interstellar clouds.

$ff = 0.6\%$. Different definitions of what constitutes a cloud and selection effects in the respective data samples probably explain the discrepancy.

In our random clump production, we attempted to generate a medium that resembles the interstellar medium in as many features as possible. We find the size spectrum of clouds consisting of one or more connected clumps produced in our mechanism to approach a power-law form $\rho(n) \propto n^{-\gamma}$, where γ decreases as ff increases. Such power-law forms are predicted by percolation theory (Stauffer & Aharony 1992) for filling factors near the percolation threshold $ff \approx 0.25$, and the predicted value for a three-dimensional body-centered cubic lattice is $\gamma = 2.18$. Since the clump density is identical throughout a given model, the size spectrum is equivalent to the mass spectrum of the clouds produced. Diffuse interstellar clouds appear to exhibit a mass spectrum with a value of $\gamma \approx 2$, while giant molecular clouds are described by $\gamma \approx 1.6$ (Dickey & Garwood 1989). We reproduced the form of the power law

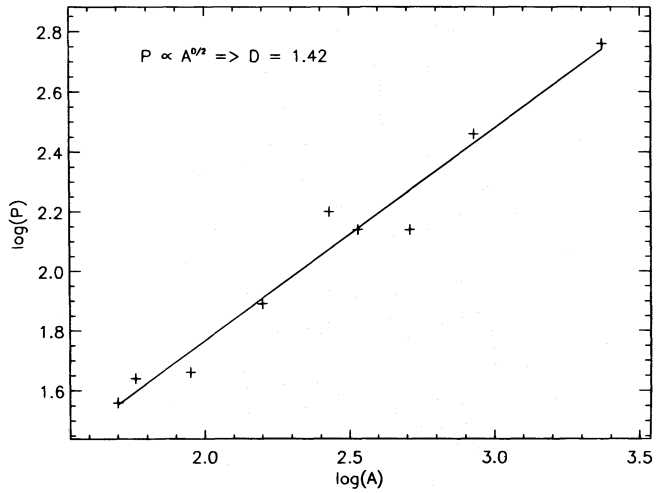

FIG. 7.—Mandelbrot's (1983) relation between the projected area A and the perimeter P of cloud structures defined by a limiting optical depth $\tau = 10$ and illustrated in Fig. 1. A fractal dimension of $D = 1.42$ is derived, similar to that observed for interstellar cloud structures.

for diffuse clouds ($\gamma = 2.11$) with a filling factor $ff \approx 0.2$, which we view, therefore, as the value most appropriate in our models, if the aim is to reproduce the interstellar cloud spectrum. In that case, our model typically represents a spiral disk environment on the scale of about $\lesssim 1$ kpc. Figure 6 shows the number of clouds as a function of number of clumps per cloud, i.e., the cloud mass, for our model with $ff = 0.20$.

2.2.4. *Cloud Structure*

It has been suggested that the structure of interstellar clouds is fractal in nature (Beech 1987; Vogelaar, Wakker, & Schwarz 1991; Falgarone et al. 1991). Also, percolation theory (Stauffer & Aharony 1992) predicts that the largest connected structure in a system at the percolation threshold is fractal. A frequently employed test is Mandelbrot's (1983) relation between projected area (A) and perimeter (P) of closed boundaries of clouds, $P \propto A^{D/2}$, where D is the fractal dimension of self-similar structures. Beech (1987) analyzed Lynds dark clouds in this manner and determined $D = 1.4$. Falgarone et al. (1991) found $D = 1.36$ for a sample of clouds defined by their ^{12}CO emission, while Vogelaar et al. (1991) found a range $1.2 < D < 1.55$ for interstellar clouds defined by their 21 cm H I emission and their thermal 100 μm emission traced by *IRAS*.

We applied the area-perimeter test to nine cloud structures defined by a line-of-sight optical depth $\tau = 10$ in the case illustrated in Figure 1. The areas were determined by weighing cutouts of paper enclosing the boundaries with a microscale, while the perimeters were obtained by numerical integration. The result is shown in Figure 7. Based on this test, our clouds have a fractal appearance, with dimension $D = 1.42$, i.e., well within the range determined by previous studies of actual interstellar structures. For a more extensive discussion of fractal characteristics of fractal sets in projections, see Pfenniger & Combes (1994).

Attempts have been made in the past to relate the existence of fractal structures with certain values of D to specific physical processes believed to be responsible for creating the structures in question (Méneveau 1989; Hentschel & Procaccia 1984; Dickman, Horvath, & Margulis 1990). In our case, the random creation of clumpy structures in three dimensions and their projection upon a spherical surface has led to fractal structures with a dimension very similar to that found among interstellar clouds. One possible interpretation of this result, therefore, is that little can be deduced from the fractal dimension of real interstellar clouds about the processes that led to their present projected appearance. We are not suggesting that our model distribution of clumpy structures is an actual representation of the interstellar medium, but it is a suitable approximation that reflects some of the observed characteristics of interstellar clouds. This will be of particular importance when such models are incorporated into the study of radiative transfer in galaxies with a clumpy interstellar medium (Witt & Gordon 1996b).

3. THE PHOTOMETRIC CHARACTERISTICS OF A CLUMPY SCATTERING SYSTEM

3.1. *Definitions*

Radiation will emerge from our clumpy system in three forms: partially attenuated direct stellar radiation, singly or multiply scattered light, and energy emitted as thermal radiation or luminescence by dust, after it has been absorbed

from the ambient stellar radiation field. Following the discussion by Witt et al. (1982), we define the luminosity of the system due to scattering as

$$L_N = L_* P_S P_{ES} , \quad (1)$$

where L_* is the unattenuated luminosity of the central source, P_S is the probability that stellar photons are scattered precisely once in the clumpy volume, and P_{ES} is the probability that once-scattered photons escape through the outer boundary of the volume. Thus, P_S is the probability that stellar photons are converted into diffuse photons, which occurs upon the first scattering. The probability for possible subsequent scatterings (0, 1, 2, ...) is contained in P_{ES}. The clumpy spherical medium is characterized by an effective radial optical depth τ_{eff} (which is defined in § 2.2.1) derived from the attenuated direct stellar radiation, L_{AT}, integrated over the outer spherical surface. The probability that stellar photons are scattered once anywhere in the system, averaged over many photons, is then

$$P_S = a(1 - e^{-\tau_{eff}}) , \quad (2)$$

where a is the dust albedo for single scattering. The probability that these once-scattered photons escape from the system, P_{ES}, is most sensitively dependent upon the structure of the medium and must be evaluated case-by-case via the Monte Carlo radiative transfer code.

We further define the total probability P_{EST} for the escape of stellar photons, be they direct or scattered, as

$$P_{EST} = P_S P_{ES} + e^{-\tau_{eff}} . \quad (3)$$

This permits us, then, to define the ratio of the system's emission by dust (thermal and luminescence) to optical emission (stellar and scattered) as

$$\frac{L(\mathrm{IR})}{L(\mathrm{OPT})} = \frac{(1 - P_{EST})}{P_{EST}} . \quad (4)$$

In the following discussions, we will compare the characteristics of clumpy distributions of constant mass with predictions for homogeneous spherical systems covering a wide range of albedos and radial optical depths.

3.2. *Nebular to Stellar Luminosity Ratio*

It follows from equation (1) that the ratio L_N/L_* is the product of two probabilities, P_S and P_{ES}. The former increases with optical depth, with $P_S = 0$ at $\tau_{eff} = 0$, while the latter decreases with increasing optical depth. As shown by Witt et al. (1982), $P_S \times P_{ES}$ reaches a maximum at some intermediate optical depth, the value of which depends mainly on the dust albedo but is generally in the range $1 < \tau < 3$. We illustrate the behavior of a clumpy medium with a equivalent homogeneous radial optical depth $\tau_H = 10$ in Figure 8. While keeping the total mass constant, we explore the effect of varying the filling factor of clumps upon the ratio L_N/L_*. The clump size is 1/10 of the radius, i.e., $N = 20$. The density ratio, k_2/k_1, of interclump to clump medium was varied over the range $1 \geq k_2/k_1 \geq 10^{-3}$, stepped by factors of $(10)^{1/2}$, for each series of models of given filling factor *ff*. Several observations can be made:

1. As expected from the results shown in Figure 3, the effective optical depth τ_{eff} is greatly reduced with increased density contrast between clumps and the interclump medium. Our results confirm the earlier calculations by Boissé (1990) and Hobson & Scheuer (1993) in this respect.

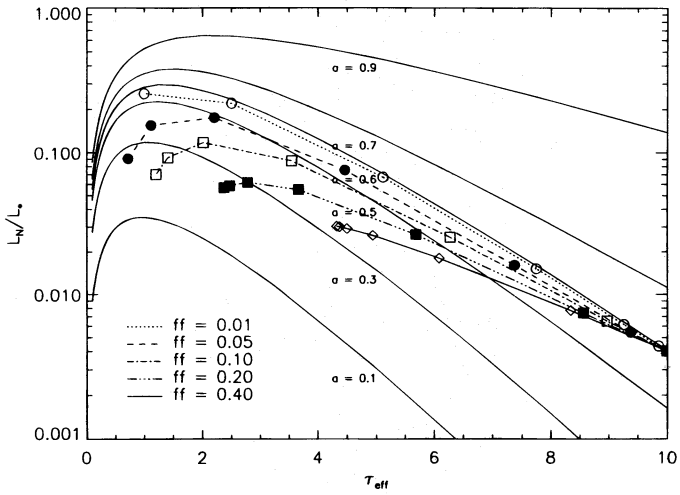

FIG. 8.—Ratio of the scattered luminosity L_N, emerging from the system, to that of the central source luminosity L_* for a range of clumpy distributions with different filling factors is being compared to homogeneous distributions with identical effective optical depths. The homogeneous models are represented by solid lines, each labeled with the dust albedo ($0.1 \leq a \leq 0.9$). All clumpy models are for an equivalent homogeneous optical depth of $\tau_H = 10$ and $N = 20$. Each sequence of models of a fixed filling factor are computed for a range of density ratios ($1 \geq k_2/k_1 \geq 0.001$) in steps of factors of 3.16, beginning at $\tau_{eff} = 10$ on the $a = 0.6$ line.

2. The scattered luminosity increases sharply by factors of 10–50 between the homogeneous case and the extremely clumpy cases. This is due to the increase in the probability P_{ES} with declining τ_{eff}, while the probability P_S remains large. This result is, however, strongly dependent on the value of τ_H. If τ_H were smaller, say $\tau_H \leq 1.5$ for $a = 0.6$, the scattered luminosity would decrease with increasing clumpiness.

3. By comparing the solution for clumpy cases with the homogeneous solutions of constant albedo (*solid lines*), we can determine the effective albedo of dust in the clumpy media. We define the effective albedo as the albedo of dust in an equivalent homogeneous system, with an optical depth equal to the effective optical depth τ_{eff}, which yields the same value of L_N/L_*.

As expected, the effective albedos of clumpy media will always be lower than the actual albedos of the grains responsible for the scattering (Boissé 1990, 1991). This is because of the multiple scattering within optically thick clumps that results in enhanced absorption. Figure 8 illustrates the important role of the interclump medium as well as the influence of the optical depth of individual clumps. For very small filling factors, the clumps are important only by incorporating mass, leaving a more transparent interclump medium to scatter with a high effective albedo and a much reduced τ_{eff}. Initially, higher filling factors lead to lower effective albedos, reflecting simply the number density of clumps; ultimately, at extreme values of k_2/k_1 of 10^{-3}, the lowest effective albedo appears for $ff = 0.1$, while larger filling factors, e.g., $ff = 0.4$, again show higher effective albedos. In this range, clumps dominate the scattering, and the greater optical depth of clumps in the $ff = 0.1$ case compared to the $ff = 0.4$ case determines the lower albedo of the former case.

The length scale of clumping in our model was determined by the number of bins with potential clumps per radius. Since the effective optical depth τ_{eff} of the system

and the optical depth of the clumps depends on the clump size (§ 2.2.1), we now expect that the system's scattered luminosity will do so as well. Figure 9 shows the result of calculations for the case of $\tau_H = 10$, with $ff = 0.1$ but with a range of clump sizes, which are inversely proportional to the number of bins. For each value of k_2/k_1, the case with the largest clump size, i.e., the smallest number of bins per radius, has the lowest effective optical depth, despite the fact that both τ_1 and τ_2, the optical depths of bins filled with clump and interclump medium, respectively, are largest. The variations of τ_1 and of τ_2 with ratio k_2/k_1 are shown in Figures 10 and 11, respectively. Figures 9, 10, and 11 illustrate the fact that in a structured medium with optically thick clumps, it is not so much the optical depth of clumps but rather the covering factor, i.e., the fraction of 4π sr of solid angle filled by clumps as seen by the source, which determines the effective optical depth. For constant mass and constant filling factor, the smaller the typical clump size relative to the size of the system, the higher the covering factor. We demonstrate this in Figure 12, where we show the fraction of 4π sr covered by one or more high-density clumps as a function of clump size, which is inversely proportional to N.

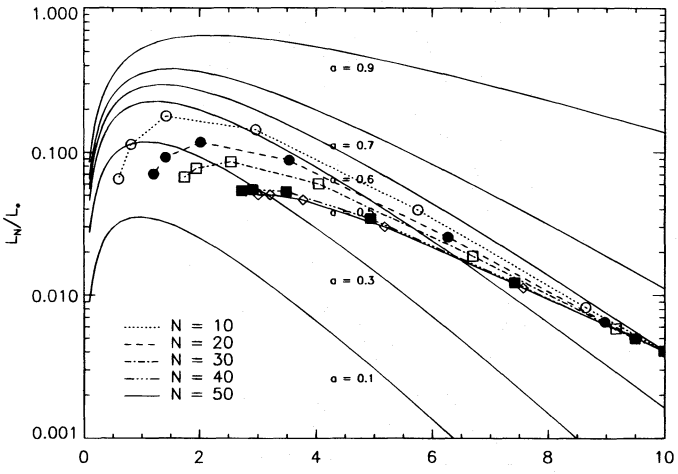

FIG. 9.—Same as Fig. 8, but for constant filling factor $ff = 0.1$ and for a range of bin sizes ($\propto 1/N$).

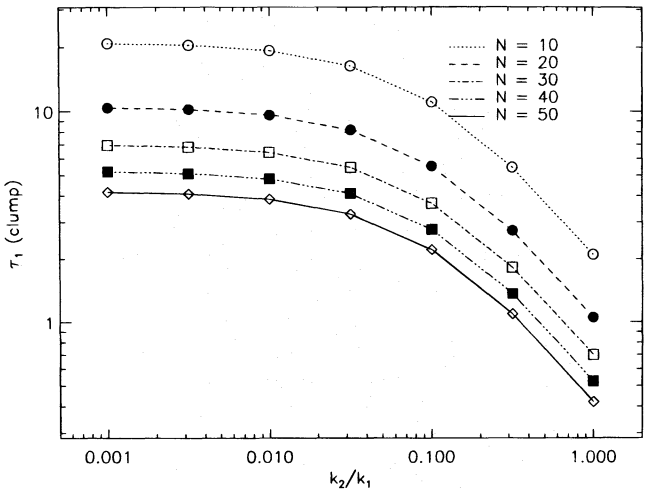

FIG. 10.—Dependence of the clump optical depth τ_1 per bin as a function of the density contrast k_2/k_1 for a range of clump sizes ($\propto 1/N$) is shown for the cases illustrated in Fig. 9. The filling factor is $ff = 0.1$.

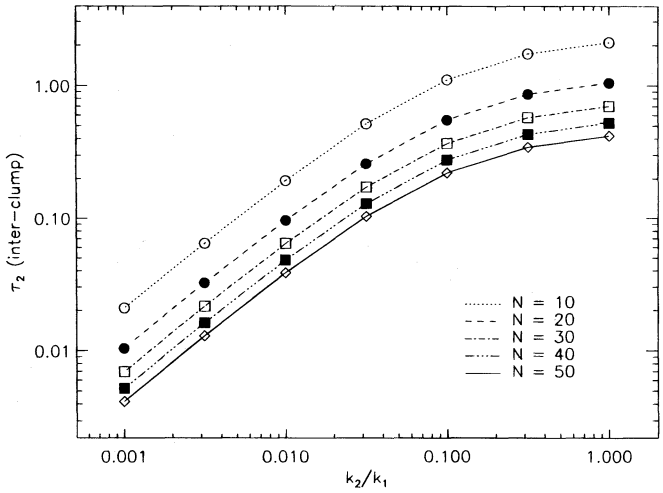

FIG. 11.—Same as Fig. 10, except for the optical depth τ_2 per bin of the interclump medium.

3.3. *The Ratio of Scattered to Direct Stellar Flux*

While the introduction of structure allows the escape of a vastly greater scattered light flux, e.g., increases by about a factor of 50 in the examples shown in Figures 8 and 9, the increase in the escape of direct stellar flux is considerable greater, going as $e^{-\tau_{\rm eff}}$. Consequently, the ratio of scattered to direct stellar flux from the system, F_N/F_*, recorded and averaged by an external integrating sphere encasing the system decreases monotonically as the ratio k_2/k_1 decreases. We illustrate the case for $\tau_H = 10$ and $ff = 0.1$ for different clump sizes in Figure 13. The ratio F_N/F_* is determined to first order by the effective optical depth of the system, but it is always lower than the equivalent homogeneous case of constant albedo, where the optical depth is replaced by $\tau_{\rm eff}$. This reflects the reduced scattering efficiencies of clumps the effective albedo of which is always lower than that of the grains contained within them. The effective albedo

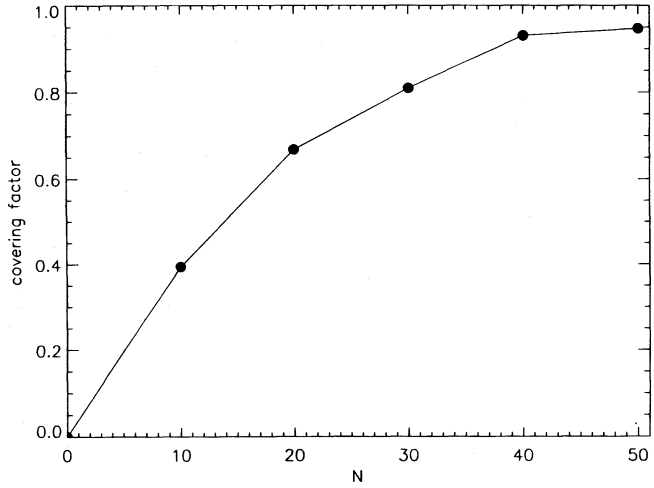

FIG. 12.—Fraction of 4π sr covered by one or more high-density clumps as seen from the central source, as a function of N. The size of individual clumps is $\propto 1/N$, the case illustrated is for $ff = 0.1$.

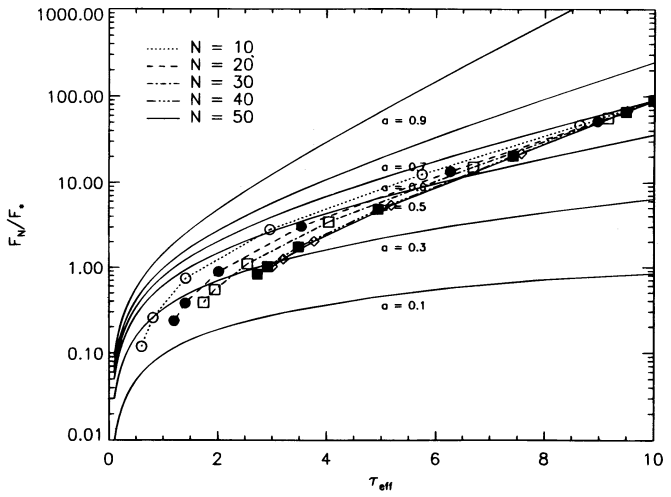

FIG. 13.—Flux ratio of scattered to direct stellar radiation as observed by an outside observer for the same cases as illustrated in Fig. 9.

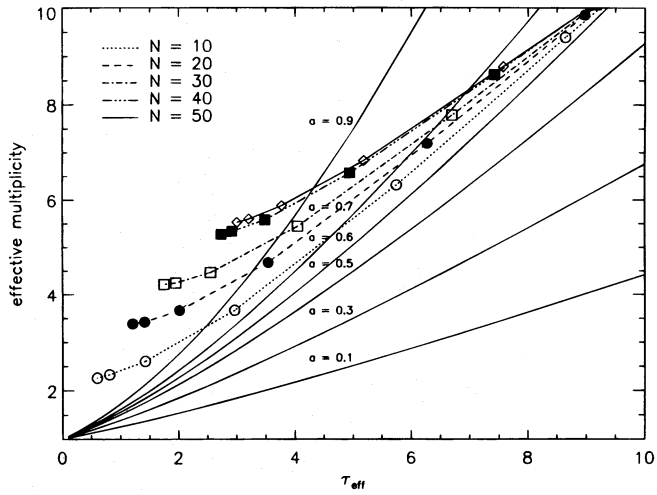

FIG. 14.—Effective multiplicity of scattering for the clumpy distribution illustrated in Fig. 9 is compared to predictions for homogeneous distributions (constant density) of dust of identical effective optical depth (*solid lines* for albedo values $0.1 \leq a \leq 0.9$).

of the scattering medium at maximum density contrast of $k_2/k_1 = 10^{-3}$ is reduced from 0.6 to values in the range 0.2–0.3. We note the ratio F_N/F_* is randomly direction-dependent and can therefore not be determined observationally for a single system. However, the ratio F_N/F_* may become a valid observational parameter when derived from an unbiased sample of many systems.

3.4. *The Effective Multiplicity of Scattering*

Although the effective optical depth of a structured medium can appear greatly reduced compared to a homogeneous case of equal mass, the history of scattered photons is strongly affected by their encounters with dense clumps. Escape from such clumps, on average, requires repeated scatterings. We measured this effect by calculating the effective multiplicity of scattering for the system (Witt 1977b),

$$m_{\rm eff} = \frac{\log\left(\sum_i^N a^{n_i}/N\right)}{\log\left(a\right)} . \qquad (5)$$

Here, N is the total number of photons in a given model calculation, n_i is the number of times the ith photon was scattered before escaping, and a is the single-scattering albedo. The effective multiplicity $m_{\rm eff}$ is a sensitive indicator of multiple scattering in Monte Carlo radiative transfer calculations, in fact more sensitive than the mean number of scatterings (Witt & Oshel 1977). Figure 14 displays results for a case with $\tau_H = 10$, $a = 0.6$, and $ff = 0.1$ for different clump sizes. As expected, the effective multiplicity is substantially in excess of that expected for homogeneous cases with $\tau = \tau_{\rm eff}$ for the same albedo. Large clumps, which provide the smaller covering factor (Fig. 12), allow photons to escape more easily, while smaller, more numerous clumps with identical total mass and filling factor, require more frequent scatterings. Since their covering factor is much higher, multiple scattering *between* clumps becomes an important factor.

The principal observational consequence of a high value of $m_{\rm eff}$ is a reduction in the degree of polarization of the scattered light emerging from a clumpy medium, compared to expectation based on homogeneous models computed for the same effective optical depth (Code & Whitney 1995). We expect to pursue this line of investigation in a future paper devoted to reflection nebulae with clumpy scattering media (Witt & Gordon 1996c).

3.5. *The Radial Distribution of the Scattered Light Intensity*

The radial surface brightness distribution of the scattered light of our clumpy spherical system will, in contrast to that of a homogeneous system, depend on the viewing direction and the position angle along which the radial light distribution is determined. In order to facilitate comparison of different cases, we therefore carry out averages over all viewing directions and position angles. While observationally it is *not* possible to average over viewing direction, it is possible to average over position angles by forming azimuthal averages over all data at fixed projected radii. The effects of clumpiness on the surface brightness distribution are best studied with large clumps, which implies smaller covering factors (see Fig. 12), rather than with smaller but more numerous clumps. Larger but fewer clumps allow the comparison of the effects of scattering by the interclump medium and the clumps to be made, and we will do so for cases illustrating optically thick systems and optically thin systems.

Figure 15 illustrates surface brightness distributions predicted for an optically thick system of $\tau_H = 10$, $ff = 0.10$, and five bins per radius ($N = 10$). The covering factor is $\sim$40% (Fig. 12), and the optical depth per clump varies between $\tau_1 = 2.1$ for $k_2/k_1 = 1.0$ and $\tau_1 = 21$ for $k_2/k_1 = 10^{-3}$ (Fig. 10). With clumps being individually optically thick, the escaping radiation is primarily affected by the opacity of the interclump medium (Fig. 11).

Two characteristics of the surface brightness distributions are of interest: the normalized surface brightness level (S_N/L_*), and the shape of the intensity distribution at small offset radii. The average level of the surface brightness distribution (S_N/L_*) is closely linked to the ratio (L_N/L_*), shown in Figure 9 for the case of five bins per radius as well as other cases. Figure 9 leads us to expect an increase in the surface brightness by about 2 orders of magnitude as the transition from $k_2/k_1 = 1.0$ to $k_2/k_1 = 0.01$ is made. This is indeed confirmed by the data shown in Figure 15. This figure also shows that the surface brightness distribution is

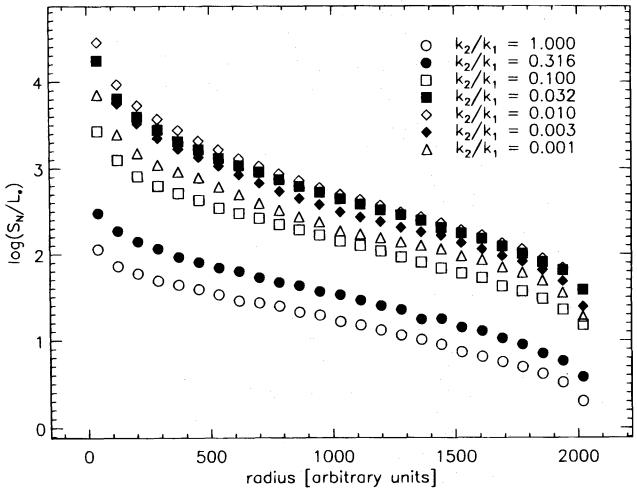

FIG. 15.—Radial surface brightness distributions of scattered light, averaged over all viewing directions, of spherical clumpy dust distributions with a central source are shown. The case illustrated has an optical radius $\tau_H = 10$ for the equivalent homogeneous case, a filling factor of 0.1, and $N = 10$.

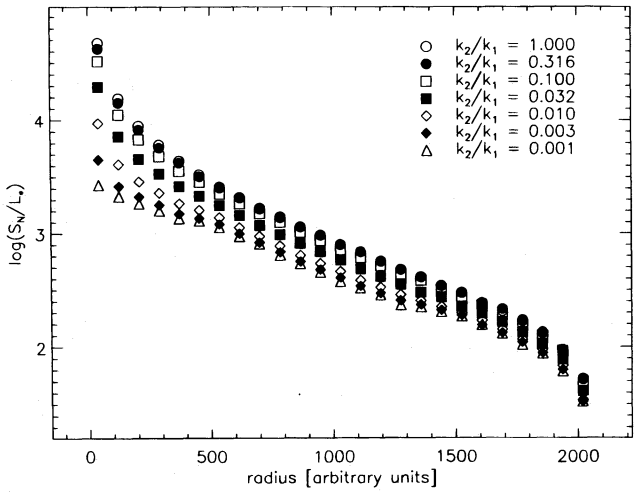

FIG. 16.—Same as Fig. 15, but for the optically thin case, $\tau_H = 1.0$

much more centrally peaked for $k_2/k_1 = 0.01$ than it is for $k_2/k_1 = 1.0$. This can be understood as the result of strongly peaked forward scattering by the optically thin interclump medium, with single scattering dominating near the star, for the case of $k_2/k_1 = 0.01$. By contrast, the homogeneous case of $k_2/k_1 = 1.0$ will permit escape of photons only after numerous scatterings even at small offsets near the star, and this will destroy the memory of the shape of the scattering phase function.

The decline in the surface brightness level between cases of $k_2/k_1 = 0.01$ and $k_2/k_1 = 0.001$ (also apparent in Fig. 15) is due solely to the decline of optical depth in the interclump medium in the optically thin limit. The surface brightness distribution remains extremely sharply peaked at zero offset, as long as single scattering by the interclump medium is the source of the diffuse photons. From Figure 11, we deduce that the optical depth through the interclump medium corresponding to the radius of our system amounts to $\sum \tau_2 = 1.00$ for $k_2/k_1 = 0.01$ and $\sum \tau_2 = 0.10$ for $k_2/k_1 = 0.001$.

If an initially optically thin system with $\tau_H = 1.0$ is turned into a clumpy structure, an entirely different behavior results, as illustrated in Figure 16. The system is most efficient in scattering in its uniform state ($k_2/k_1 = 1.0$), and it also exhibits the sharply peaked surface brightness distribution, reflecting the shape of the phase function for single scattering. Dividing the available matter into clumps reduces the overall scattering ability of the system, and the only significant scatterings occur within clumps, which implies multiple scatterings in denser structures. As a result, the surface brightness distribution loses its sharp central peak, as is evident for the case $k_2/k_1 = 0.001$ in Figure 16.

An interesting application of these results may be found in the interpretation of surface brightness observations of reflection nebulae in the optical and the near-IR spectral regions (Sellgren et al. 1992; Sellgren, Werner, & Allamandola 1995). The extinction optical depths in the V band and in the K band differ by about a factor of 10, as represented by the cases shown in Figures 15 and 16 (Savage & Mathis 1979).

In their study of scattered light in the reflection nebulae NGC 2023 and NGC 7023, Sellgren et al. (1992) found the scattered intensity in the K band to be much higher than expected for optically thin nebulae, with a ratio of optical depths $\tau_V/\tau_K \approx 10$. Yet, the surface brightness in V suggested a relatively small effective optical depth, and the surface brightness profile near the illuminating star exhibits the sharp steepening expected when single scattering dominates. The comparison of the profiles shown in Figures 15 and 16 explains this behavior fully; for ease of comparison, we plot the difference between corresponding profiles for $\tau_H = 10.0$ and $\tau_H = 1.0$ in Figure 17. We find that the clumpy distributions with $0.003 \leq k_2/k_1 \leq 0.032$ produce surface brightness distributions where the $\tau_H = 10$ case is brighter than or equal to the $\tau_H = 1$ case. Here, the $\tau_H = 10$ case, where scattering in the interclump medium dominates, has the characteristics of an optically thin nebula, while the $\tau_H = 1.0$ case, with effective scattering by clumps only, has the flatter distribution characteristic of an optically thick nebula. Clumpiness can thus induce appearances which are quite counterintuitive.

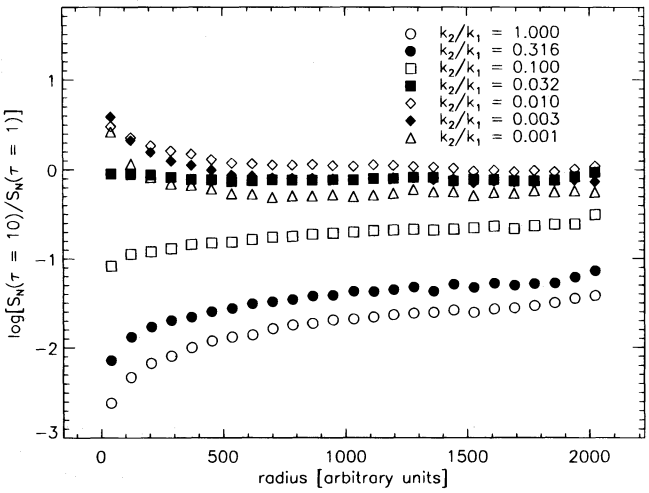

FIG. 17.—Ratios of corresponding surface brightness distributions among the $\tau_H = 10$ cases and the $\tau_H = 1.0$ cases, which were illustrated in Figs. 15 and 16, respectively.

3.6. *Conversion of Optical Light into Far-Infrared Emission*

Any photon that does not escape directly or after one or more scatterings will be absorbed within the system. Since dust is the dominant source of opacity, the overwhelming fraction of the absorbed energy re-emerges as thermal dust emission in the mid- and far-infrared and submillimeter regions of the spectrum. In § 3.1 we identified the ratio $(1 - P_{EST})/P_{EST}$ as corresponding to the ratio of the far-IR thermal radiation to the observable UV/optical light of the system, F_{IR}/F_{OPT}.

In Figure 18 we show the variation of this ratio with contrast between clump and interclump medium ($0.001 \leq k_2/k_1 \leq 1.0$) for a case of $\tau_H = 10$ and $ff = 0.10$, for a range of clump sizes. The structure of the medium is extremely influential; we observe a range of variation by a factor of order 250 among the cases illustrated in Figure 18, which as before contain the same identical dust mass in each instance. Increasing the density contrast between clumps and the interclump medium and the formation of larger rather than smaller clumps lead to the greatest reduction in the ratio F_{IR}/F_{OPT}. Under no circumstances should the ratio F_{IR}/F_{OPT} be used to infer the mass of dust present in a dusty system, unless the structure of the dusty medium can be described fully.

The observed range of F_{IR}/F_{OPT} in infrared-luminous galaxies (Witt et al. 1992b) or in dusty spiral disk galaxies (Xu & Buat 1995) can in part be explained as resulting from structures of the ISM deviating by different degrees from the homogeneous state. Most IR-luminous galaxies appear to be the result of gravitational interactions or mergers among galaxies (see, e.g., Sanders et al. 1988). The results shown in Figure 18 suggest that the destruction of large cloud complexes into more numerous smaller clouds, i.e., N increasing, and the dispersion of smaller clouds within the diffuse intercloud medium, i.e., k_2/k_1 increasing, can easily lead to the dramatic increase in infrared emission seen from such objects. Other phenomena, such as the formation of massive stars inside molecular clouds and the dispersal of clouds within an extended star distribution, may of course contribute in an equally important manner.

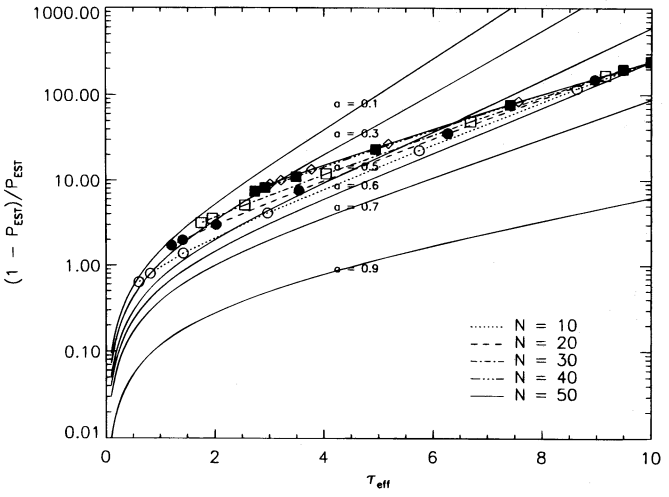

FIG. 18.—Function $(1 - P_{EST})/P_{EST}$, which is equivalent to the ratio of far-IR thermal luminosity to UV/optical/near-IR direct stellar and scattered light luminosity for a dusty stellar system, is shown here for homogeneous systems (*solid lines* for albedo values $0.1 \leq a \leq 0.9$) and for a clumpy dust distribution for a range of density contrasts ($0.001 \leq k_2/k_1 \leq 1.0$) and a dust albedo of $a = 0.6$. Successive points of a given clump size ($\propto 1/N$) are for conditions differing in k_2/k_1 by factors of 3.16.

4. DISCUSSION

Our model is clearly a highly simplified representation of the actual structure found in real systems, be they star-forming regions, reflection nebulae, or dusty disks of late-type galaxies. However, it does contain the basic elements of structure, two phases with different nonzero extinction coefficients, randomly shaped forms, and a mass spectrum of high-density clumps similar to that found in the Galaxy. The effect of such structure on the transfer of radiation produces clear and systematic differences compared to homogeneous media (see Natta & Panagia 1984; Boissé 1990; Hobson & Scheuer 1993). Models employing homogeneous media for objects in which the assumption of homogeneity is clearly inappropriate and unsupported by observations thus lead to strongly biased conclusions. Such biases are more pronounced, the higher the value of the extinction coefficient. Specific instances of such biases affect determinations of opacities of interstellar regions, of albedos of interstellar grains at different wavelengths, and of dust masses present in stellar systems. With an opacity law similar to that of the average interstellar extinction law in the Galaxy, biases will affect ultraviolet radiation more strongly than longer wavelength radiation, because clumps will approach optical thickness first at the shorter wavelengths. As long as clumps are individually optically thin, the effects of structure are minor.

4.1. *Scaling of Effective Optical Depths*

It is always true that the effective optical depth of a clumpy system is less than that of the equivalent homogeneous system of equal mass. This was demonstrated convincingly by Boissé (1990) and Hobson & Scheuer (1993) for the case of a plane-parallel clumpy slab. The details of this reduction depend on the density ratio (k_2/k_1) of the two phases, the filling factor, the size of the clumps relative to the system as a whole, and the distribution of the sources relative to the dust in cases in which multiple sources are present (Witt & Gordon 1996b). The differences between a clumpy system and an equivalent homogeneous one are clearly maximized, if all sources are concentrated at the center, as has been assumed for the cases described in this paper.

We illustrate the dependence of the effective optical depth on the density contrast between the two phases of the scattering medium in Figure 19. This is a case with $N = 20$ in which the mass scales in direct proportion to τ_H. As expected, the effective optical depth of the medium does *not* scale linearly with the amount of dust present, represented by the equivalent optical depth τ_H of a homogeneous dust distribution. This was previously shown by Natta & Panagia (1984) for a clumpy screen with zero-density interclump medium and Boissé (1990) for the more general two-phase slab. For a given clump size, the nonlinearity as well as the reduction in effective optical depth become more pronounced as the density contrast between the two phases increases. This occurs for the simple reason that clumps, once optically thick, produce opacity by blocking radiation. The covering factor and the ability of radiation to escape through interclump space without suffering significant extinction are then determining factors for this type of opacity.

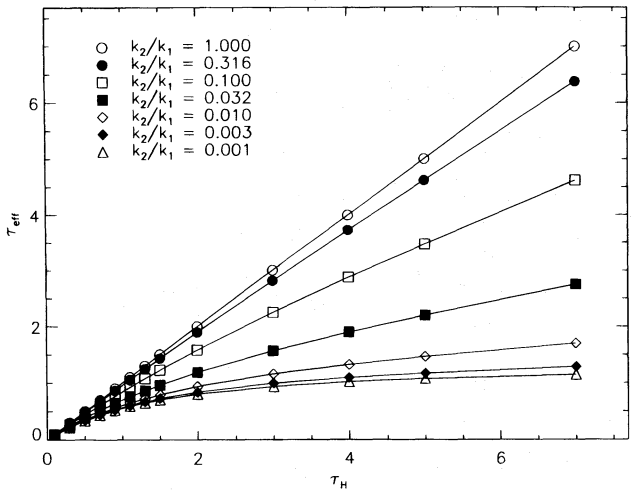

FIG. 19.—Scaling of the effective optical depth τ_{eff} of clumpy systems for different density contrasts k_2/k_1 with the radial optical depth τ_H of systems with equal mass homogeneous dust distributions.

We can anticipate several interesting observational consequences to arise from this behavior. Let us assume that the dust in galaxies exhibits an extinction law equal to that of the average Galactic extinction. The results of Figure 19 suggest that the attenuation of the integrated light of such galaxies due to embedded dust with a clumpy structure will show a wavelength dependence considerably flatter in the UV than would be suggested by the average Galactic extinction curve. Structures in the far-UV extinction, such as the 2175 Å bump and the secondary minimum near 1800 Å (Savage & Mathis 1979), will be greatly smoothed out. Such behavior should be most extreme when sources are deeply embedded in dust, when the clumps are relatively large, and when the interclump spaces are comparatively empty. It requires further study to see whether the apparent absence of the 2175 Å bump in the internal dust attenuation laws of starburst galaxies (Calzetti, Kinney, & Storchi-Bergmann 1994) is due solely to this mechanism.

4.2. *Reddening by Clumpy Media*

In their study of radiative transfer in galactic environments, Witt et al. (1992b) showed that extended star distributions filled with a homogeneous scattering interstellar medium approach finite limiting reddening values with increasing dust mass, once conditions of optical thickness are obtained. This saturation of reddening from an extended distribution is caused by the fact that the observed light at each wavelength comes from a region $\tau \approx 1$ or less, and the ratio of the volumes of such regions at different wavelengths approaches a constant as the dust mass increases.

As the data shown in Figure 19 clearly suggest, a clumpy dust distribution will produce even less reddening in a given geometry with an extended source distribution than a homogeneous one (see, e.g., Natta & Panagia 1984). As dust is concentrated in clumps, these will become optically thick much more quickly than the equivalent homogeneous distribution would. Consequently, the reddening of the integrated light of a galactic environment should approach even lower saturation values, well below those expected for homogeneous dust distributions. For a given mass of dust, the larger the individual clumps, the greater their optical depth, the less reddened the integrated light. We anticipate, therefore, that the reddening of the light emanating from a star-forming region, for example, is not determined just by the amount of dust or kind of dust present or by the dust-star geometry but, rather, probably most strongly by the prevailing structure of the dusty medium.

4.3. *Change of ISM Structure in Interacting Galaxies*

Interacting or merging galaxies not only are frequently exceptionally luminous (see, e.g., Sanders et al. 1988), but they also have, as a class, a higher ratio of infrared to optical luminosity (Braine & Combes 1993). This behavior is normally attributed to bursts of star formation occurring in conjunction with mergers or gravitational interactions (Bushouse 1987; Fritze–v. Alvesleben & Gerhard 1994). However, while star formation will lead to increases in both UV–optical radiation and infrared (thermal) dust emission, it does not necessarily follow that the *ratio* of infrared to optical radiation should increase as well, at least not for long. If the interstellar medium is clumpy, Figure 19 suggests that the effective opacity in the UV, where most of the newly formed stellar emission would occur, is not much higher than it is in the visible or near-IR. The increased opacity needed for effective conversion of optical/UV radiation into far-infrared thermal emission can be obtained, however, from a change in the structure of the ISM. We suggest, therefore, that mergers and gravitational interactions involving galaxies are associated with bursts of star formation and a breakup of large interstellar cloud complexes into numerous smaller clouds and a intercloud medium of enhanced density. As demonstrated in Figure 18, this dispersal of the ISM would lead to a greatly enhanced conversion efficiency from UV/optical light into far-IR thermal radiation. This has been shown in more detail in Witt & Gordon (1996a).

Independent confirmation of this suggested structure comes from an unusually low ratio of $^{13}CO/^{12}CO$ in interacting galaxies compared to normal spirals (Aalto et al. 1991). A likely explanation is small clouds ($\lesssim 1$ pc), in which ^{12}CO as well as ^{13}CO would be observable under optically thin conditions. A greater velocity dispersion of an existing cloud distribution could also contribute to this observational result. The resulting increased spatial dispersion leads to a greater effective opacity as well. The analysis of far-IR fine-structure lines in the starburst galaxies NGC 253 and NGC 3256 by Carrel et al. (1994) leads to very similar conclusions regarding the structure of the ISM in those systems.

4.4. *Bias in Dust Albedo Determinations*

The scattering response of a clumpy system is consistently that of an equivalent system of lower effective optical depth and lower effective albedo (see Figs. 8, 9, and 13). The apparent reduction of the albedo may be seen as arising from the fact that clouds of dust grains replace individual grains as the effective scatterers (see also Hobson & Padman 1993). Multiple scattering occurring within clouds leads to increased absorption and thus reduces the amount of scattered light leaving the cloud surfaces. We illustrate this effect by computing the effective albedo of spherical clouds with radial optical depths of 0.2, 1.0, and 5.0, with dust of albedo = 0.6, shown in Figure 20. This calculation is based on the integrated scattered light returned by uniform spherical clouds embedded in an isotropic radiation field.

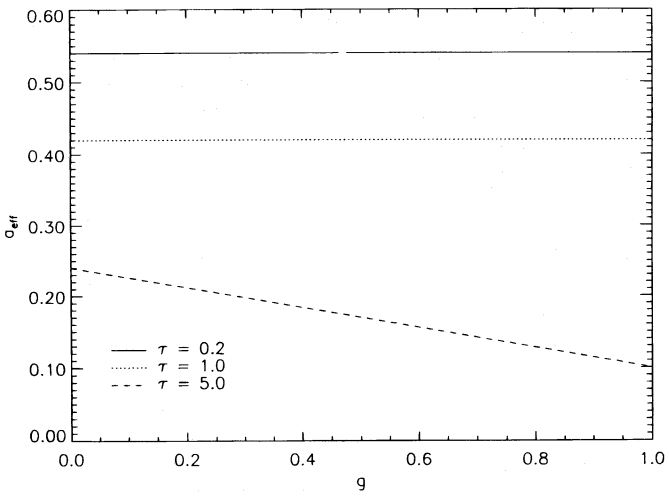

FIG. 20.—Effective albedo of spherical, externally illuminated clouds, containing dust with a single-scattering albedo $a = 0.6$, as a function of the phase function asymmetry parameter g. Three cases for $\tau = 0.2$, 1.0, and 5.0 are indicated, where τ is the radius of the clouds in optical depth space.

As long as the clouds are not fully opaque ($\tau = 0.2$ and 1.0), the effective albedo is independent of the phase function asymmetry g; there is, however, a significant reduction in the effective albedo even for clouds with relatively small τ, on the basis of their optical depth alone, by 10% and 30% for $\tau = 0.2$ and $\tau = 1.0$, respectively. These values agree reasonably well with results obtained from an analytical approximation by Boissé (1990). For opaque clouds ($\tau = 5$), the dependence of the effective optical depth upon the phase function asymmetry becomes pronounced. Larger values of g, corresponding to a more strongly forward-directed phase function, lead to photons being directed toward the opaque cloud interior, where their chance of survival as scattered photons is greatly diminished. This effect may have significant consequences for attempts to derive scattering properties of dust grains in systems for which the dust distribution is clumpy. This is particularly serious in spectral regions in which the optical depth rises rapidly, e.g., shortward of 1600 Å (Witt et al. 1993) and in which there are strong indications that the phase-function asymmetry increases simultaneously. Thus, the study of NGC 7023 (Witt et al. 1992a, 1993), which indicated a declining dust albedo with decreasing wavelength shortward of 1300 Å, may have been biased by the demonstrated presence of clumpy structure (see § 3.5).

5. SUMMARY

The clumpy structure of diffuse media in astronomical systems has a profound impact upon the transfer of radiation through such media and the escape of stellar and scattered radiation from such media. In this paper, we have studied the very simple case of a central source surrounded by a spherical, statistically homogeneous but clumpy two-phase scattering medium. The main focus has been upon systems of constant mass in which the dust distribution was variable, i.e., variable interclump-to-clump density ratio, clump size, and filling factor of clumps. The source of opacity was scattering by dust grains of constant albedo $a = 0.6$ and a strongly forward-directed phase function asymmetry parameter $g = 0.6$.

Our principal conclusions are the following:

1. A minimum of two phases of nonzero density, in contrast to a system of clumps in vacuum, is necessary for the adequate description of a clumpy medium, as was shown previously by Boissé (1990) and Hobson & Scheuer (1993). The low-density interclump medium and the denser clumps contribute to the opacity of the system generally in different ways. Optically thick clumps mainly block radiation, an effect governed by the filling factor, while the scattering by the optically thinner interclump medium is dependent upon the integrated optical depth to the system surface through this interclump phase.

2. The presence of random structure in a medium leads to a reduction of the overall effective opacity of that medium, as was shown previously by Boissé (1990) and Hobson & Scheuer (1993). This tends to result in underestimates of the density and mass of the dust present in systems suffering from dust obscuration.

3. The production of clumps via a random process leads to a cloud mass spectrum with a power law $N(M) \propto m^{-2.1}$, very similar to that observed for diffuse clouds in the Galaxy, provided the filling factor is also chosen close to that observed, i.e., $ff = 0.2$. This result was expected from general predictions of percolation theory (Stauffer & Aharony 1992) and confirmed by our model. Such cloud structures appear in projection as fractal in nature with a fractal dimension $D \simeq 1.4$, similar to that observed in the interstellar medium of our Galaxy. This finding may be of importance for the interpretation of the mass spectrum of interstellar clouds and their apparent fractal nature (Pfenniger & Combes 1994).

4. The scattered light luminosity of a system initially optically thick in the homogeneous state increases significantly when the scattering medium assumes a two-phase clumpy structure. However, the direction-averaged ratio of scattered to stellar flux seen by outside observers decreases during the same change, because the stellar flux increases more strongly than the nebular flux.

5. The effective multiplicity of scattering increases with increased density contrast between clump and interclump material compared to homogeneous media with identical effective optical depth. As a consequence, one would expect *reduced* degrees of polarization because of scattering by a clumpy medium.

6. Surface brightness distributions of scattered light may exhibit the characteristics of optically thin or optically thick cases, depending whether the principal contribution to the scattering is the interclump medium or the clumps. Thus, the same system may appear optically thin in the UV and optically thick in the near-IR, contrary to the actual ratios of the optical depths associated with those spectral regions.

7. Scattering by a clumpy medium is generally equivalent to scattering by a homogeneous medium of lower optical depth, with dust of lower albedo as long as global properties of the system are considered. Consequently, radiative transfer analyses based on homogeneous models applied to inhomogeneous systems can lead to underestimates of the dust albedo (Boissé 1990; Hobson & Scheuer 1993) and the total dust mass. However, the detailed appearance of the system from a fixed perspective is determined by the actual distribution of clumps.

8. Through its effect upon the overall effective opacity, the presence of structure in the ISM also has a profound impact upon the efficiency of converting UV/optical radiation into far-IR thermal dust emission. We suggest that the

high conversion efficiency observed in starburst galaxies and mergers is due in large part to a change in the structure of the ISM in such systems toward a more homogeneous widely extended distribution.

We acknowledge financial support from NASA LTSAP grant NAGW-3168 to The University of Toledo. This work was completed while A. N. W. was a Visitor at the European Southern Observatory in Garching. A. N. W. is grateful for the ESO hospitality and financial support. We are indebted to the referee for numerous constructive suggestions and comments, especially in regard to percolation theory.

REFERENCES

Aalto, S., Block, J. H., Booth, R. S., & Johansson, L. E. B. 1991, A&A, 247, 291
Audic, S., & Frisch, H. 1993, J. Quant. Spectrosc. Radiat. Transf., 50, 127
Beech, M. 1987, Ap&SS, 133, 193
Block, D. L., Witt, A. N., Grosbol, P., Stockton, A., & Moneti, A. 1994, A&A, 288, 383
Boissé, P. 1990, A&A, 228, 483
———. 1991, in IAU Symp. 147, Fragmentation of Molecular Clouds and Star Formation, ed. E. Falgarone et al. (Dordrecht: Kluwer), 119
Bosma, A., Byun, Y., Freeman, K. C., & Athanassoula, E. 1992, ApJ, 400, L21
Braine, J., & Combes, F. 1993, A&A, 269, 7
Bruzual A., G., Magris, G., & Calvet, N. 1988, ApJ, 333, 673
Burton, M. G., Hollenbach, D. J., & Tielens, A. G. G. M. 1990, ApJ, 365, 620
Bushouse, H. A. 1987, ApJ, 320, 49
Byun, Y.-I. 1993, PASP, 105, 993
Byun, Y.-I., Freeman, K. C., & Kylafis, N. D. 1994, ApJ, 432, 114
Calzetti, D., Bohlin, R. C., Gordon, K. D., Witt, A. N., & Bianchi, L. 1995, ApJ, 466, L97
Calzetti, D., Kinney, A. L., & Storchi-Bergmann, T. 1994, ApJ, 429, 582
Carrel, P., et al. 1994, ApJ, 423, 223
Code, A. D., & Whitney, B. A. 1995, ApJ, 441, 400
Colomb, F. R., Pöppel, W. G. L., & Heiles, C. 1980, A&AS, 40, 47
Cunow, B. 1992, MNRAS, 258, 251
Dickey, J. M., & Garwood, R. W. 1989, ApJ, 341, 201
Dickman, R. L., Horvath, M. A., & Margulis, M. 1990, ApJ, 365, 586
Falgarone, E., Phillips, T. G., & Walker, C. K. 1991, ApJ, 378, 186
Fritze–v. Alvesleben, U., & Gerhard, O. E. 1994, A&A, 285, 751
Gaustad, J. E., & van Buren, D. 1993, PASP, 105, 1127
Gordon, K. D., Witt, A. N., Carruthers, G. R., Christensen, S. A., & Dohne, B. C. 1994, ApJ, 432, 641
Han, M. 1992, ApJ, 391, 617
Hentschel, H. G. E., & Procaccia, I. 1984, Phys. Rev. A, 29, 1461
Henyey, L. G., & Greenstein, J. L. 1941, ApJ, 93, 70
Hobson, M. P., & Padman, R. 1993, MNRAS, 264, 161
Hobson, M. P., & Scheuer, P. A. G. 1993, MNRAS, 264, 145
Howe, J. E., Jaffe, D. T., Genzel, R., & Stacey, G. J. 1991, ApJ, 273, 158
Huizinga, J. E., & van Albada, T. S. 1992, MNRAS, 254, 677
Jansen, R. A., Knapen, J. H., Beckman, J. E., Peletier, R. F., & Hes, R. 1994, MNRAS, 270, 373
Mandelbrot, B. B. 1983, The Fractal Geometry of Nature (New York: Freeman)
Meixner, M., & Tielens, A. G. G. M. 1993, ApJ, 405, 216
Méneveau, C. 1989, Ph.D. thesis, Yale Univ.
Murthy, J., Walker, H. J., & Henry, R. C. 1992, ApJ, 401, 574
Natta, A., & Panagia, N. 1984, ApJ, 287, 228
Pfenniger, D., & Combes, F. 1994, A&A, 285, 94
Rosen, A., & Bregman, J. N. 1995, ApJ, 440, 634
Rowan-Robinson, M. 1992, MNRAS, 258, 787
Sanders, D., B., et al. 1988, ApJ, 325, 74
Savage, B. D., & Mathis, J. S. 1979, ARA&A, 17, 73
Scalo, J. 1990, in Physical Processes in Fragmentation and Star Formation, ed. R. Capuzzo-Dolcetta et al. (Dordrecht: Kluwer), 151
Sellgren, K., Werner, M. W., & Allamandola, L. J. 1995, preprint
Sellgren, K., Werner, M. W., & Dinerstein, H. L. 1992, ApJ, 400, 238
Spaans, M. 1994, in ASP Conf. Proc. 58, The First Symposium on the Infrared Cirrus and Diffuse Interstellar Clouds, ed. R. M. Cutri & W. B. Latter (San Francisco: ASP), 421
Stacey, G. J., et al. 1993, ApJ, 404, 219
Stauffer, D. 1985, Introduction to Percolation Theory (1st ed; London: Taylor & Francis)
Stauffer, D., & Aharony, A. 1992, Introduction to Percolation Theory (2d ed.; London: Taylor & Francis)
Stutzki, J., et al. 1991, in Fragmentation of Molecular Clouds and Star Formation, ed . E. Falgarone et al. (Dordrecht: Kluwer), 235
Valentijn, E. A. 1994, MNRAS, 266, 614
van Buren, D. 1989, ApJ, 338, 147
Vogelaar, M. G. R., Wakker, B. P., & Schwarz, U. J. 1991, in Fragmentation of Molecular Clouds and Star Formation, ed. E. Falgarone et al. (Dordrecht: Kluwer), 508
Witt, A. N. 1977a, ApJS, 35, 1
———. 1977b, ApJS, 35, 31
———. 1988, in Dust and the Universe, ed. M. E. Baily & D. A. Williams (Cambridge: Cambridge Univ. Press), 1
Witt, A. N., & Gordon, K. D. 1996a, in AIP Conf. Proc. 348, Unveiling the Cosmic Infrared Background, ed. E. Dwek (New York: AIP), 230
———. 1996b, in preparation
———. 1996c, in preparation
Witt, A. N., Oliveri, M. V., & Schild, R. E. 1990, AJ, 99, 888
Witt, A. N., & Oshel, E. R. 1977, ApJS, 35, 31
Witt, A. N., Petersohn, J. K., Bohlin, R. C., O'Connell, R. W., Roberts, M. S., Smith, A. M., & Stecher, T. P. 1992a, ApJ, 395, L5
Witt, A. N., Petersohn, J. K., Holberg, J. B., Murthy, J., Dring, A., & Henry, R. C. 1993, ApJ, 410, 714
Witt, A. N., Thronson, H. A., & Capuano, J. M. 1992b, ApJ, 393, 611
Witt, A. N., Walker, G. A. H., Bohlin, R. C., & Stecher, T. P. 1982, ApJ, 261, 492
Xu, C., & Buat, V. 1995, A&A, 293, L65